RSC Advances

ROYAL SOCIETY OF CHEMISTRY

www.rsc.org/advances

Co-delivery of doxorubicin hydrochloride and verapamil hydrochloride by pH-sensitive polymersomes for the reversal of multidrug resistance

Nuannuan Li[a], Pei Zhang [a], Chunzhi Huang[a], Yunmei Song[b], Sanjay Garg[b] and Yuxia Luan[a]*

[a]*School of Pharmaceutical Science, Shandong University, 44 West Wenhua Road, Jinan, Shandong Province, 250012, P. R. China. Fax: (86) 531-88382548; Tel: (86) 531-88382007; E-mail: yuxialuan@sdu.edu.cn*

[b]*School of Pharmacy and Medical Sciences, University of South Australia, Adelaide SA 5000*

ABSTRACT

In this paper, we synthesized the pH-sensitive and biodegradable amphiphilic polypeptide-based block copolymer methoxy-poly(ethylene glycol)$_{2K}$-poly(ε-caprolactone)$_{4K}$-poly(glutamic acid)$_{1K}$ (mPEG$_{2K}$-PCL$_{4K}$-PGA$_{1K}$). MPEG$_{2K}$-PCL$_{4K}$-PGA$_{1K}$ had low critical aggregation concentration and could self-assemble into polymersomes in aqueous solution revealed by transmission electron microscopy. Therefore, two hydrophilic drug doxorubicin hydrochloride (DOX) and verapamil hydrochloride (VER) were encapsulated into the mPEG$_{2K}$-PCL$_{4K}$-PGA$_{1K}$ polymersomes to form poly(DOX+VER) co-delivery system to reverse the multidrug resistance by inhibiting the expression of P-glycoprotein and improve the anti-cancer effect of DOX. The in vitro cytotoxicity experiments indicated the obviously higher inhibition ratio to MCF-7/ADR resistant cells of

poly(DOX+VER) compared with that of free DOX solution and polyDOX. The release rate of the two drugs from poly(DOX+VER) were much slower than that form the free drug solutions, and their release behaviors exhibited high pH-sensitive character. Furthermore, the low hemolysis ratio of $mPEG_{2K}$-PCL_{4K}-PGA_{1K} confirmed that the copolymer could be applied for intravenous injection safely. Therefore, all these findings indicated that the co-delivery of DOX and VER by $mPEG_{2K}$-PCL_{4K}-PGA_{1K} polymersomes is very promising for cancer therapy.

1. Introduction

To these days, serious side effects and multidrug resistance (MDR) have been the two most important issues for chemotherapeutic drugs such as doxorubicin hydrochloride (DOX). DOX is an effective anti-cancer drug and has been used for various tumor treatment on clinic. However, it can induce severe cardiotoxicity because of the lack of target ability,[1] which limits the dosage of administration. Though DOX-loaded drug delivery systems with target ability can send DOX into tumor issue to reduce its cardiotoxicity,[2] the MDR is still a difficult problem to overcome. DOX is known as the P-glycoprotein (P-gp) substrate[3] and it can also active the expression of P-gp.[4] The over-expression of P-gp can pump drugs out of the plasma membrane and lower the levels of drugs in the cytoplasm to decrease the anti-tumor effect.[5] Verapamil hydrochloride (VER), a kind of calcium channel antagonist, has been applied as antiarrhythmic drugs on clinic. In these years, many studies have shown that VER can also act as P-gp inhibitor to increase the

accumulation of anti-cancer drugs within the cancer cells.[6,7] It can also reduce the clearance of DOX, resulting in the increased AUC and elongated half-life.[8] However, the free VER administration can cause an additive cardiotoxicity.[9] While the VER loaded drug delivery system is able to reduce the cardiotoxicity. Therefore, the combination of DOX and VER is desirable for cancer therapy. The combination therapy using drug delivery systems mainly include two ways: 1) one drug-loaded delivery system used with another drug-loaded delivery system; 2) the (drug+drug)-loaded system which is also defined co-delivery system. It has been reported that the cardiotoxicity of VER can be obviated and the anti-cancer effect of DOX can be improved by combining the VER-loaded and DOX-loaded delivery systems (VER and DOX are loaded respectively).[10] However, the combination of the respective drug-loaded systems cannot deliver the drugs to the target sites at the same time to obtain the drug ratio as designed for guaranteeing the effective cancer therapy. Therefore, the co-delivery of DOX and VER are studied in our manuscript.

Polymersomes are self-assembled vesicles with large hydrophilic core which can load hydrophilic agents[11] such as DOX and VER. They are usually prepared by synthetic biodegradable amphiphilic block copolymers. Compared with liposome[8,12] which also possess a hydrophilic core and is prepared by lipid, the polymersomes has a much tougher membrane to guarantee the better stability. So less leakage occurs in polymersomes than that in liposomes. In addition, the polymersomes often show a high drug loading efficiency for hydrophilic drugs compared with other drug delivery

formulations.[13,14] And the physical and chemical properties of polymersomes including particle size, drug loading content, particle morphology and others can also be tuned by the molecular weight, preparation and et alia for various purposes.[15-17] On the other hands, the stable polymersomes may inhibit the release of drugs. Therefore, a stimuli-response polymersomes is desirable for delivering drugs.[18,19]

Therefore, in the present study we prepared the pH-sensitive polymersomes based on the polypeptide-based $mPEG_{2K}$-PCL_{4K}-PGA_{1K} we synthesized. MPEG and PCL are selected as hydrophilic block and hydrophobic block respectively for the good biocompatibility and non-cytotoxicity.[20-22] PGA, a kind of polypeptide which has been studied broadly for their various stimuli-responsibility[23] acts as the pH-sensitive block. Under neutral and basic conditions, the charged PGA is water soluble. At acidic pH, the neutralized PGA shows a great decrease in solubility[24]. The decrease of PGA in solubility makes the change of proportions between hydrophilic block and hydrophobic block in the copolymer which can further vary the structure of the aggregate to induce the release of drugs. In addition, it has been confirmed that the pH-sensitive PGA can facilitate the endosomal escape[25-27] and guarantee the anticancer effect of drugs. Therefore, the pH-sensitive $mPEG_{2K}$-PCL_{4K}-PGA_{1K} polymersomes is desired to improve the accumulation of drugs in acidic tumor issue and decrease the concentration of drugs in blood, improving the anti-cancer effect and decreasing the cardiotoxicity of the anticancer drugs.

Based on the theories mentioned above, we prepared the pH-sensitive poly(DOX+VER) co-delivery systems for the reversal of MDR and high anti-cancer effect. The polypeptide-based block copolymer $mPEG_{2K}$-PCL_{4K}-PGA_{1K} was synthesized by ring-opening polymerization (ROP) and characterized by ^{1}H NMR. And it could assemble into polymersomes in aqueous solution spontaneously with appropriate particle size for targeting tumor issue via enhanced permeability and retention (EPR) effect.[28] The hydrophilic drug DOX and VER were physically encapsulated into the polymersomes via the simple dialysis method. The release test *in vitro* conducted in pH 7.4 and pH 5.0 PBS buffer indicated that the polymersomes co-delivery systems showed a high pH-sensitivity and sustained release ability. The *in vitro* cytotoxicity and cellular uptake were evaluated in MCF-7 and MCF-7/ADR resistant cells, and the results confirmed that the poly(DOX+VER) could effectively reverse MDR and improve the anti-cancer effects significantly.

2. Research methods

2.1 Materials

Methoxy-poly(ethylene glycol) ($mPEG_{2K}$) was purchased from Sigma-Aldrich; ε-caprolactone, stannous octoate, dicyclohexylcarbodiimide (DCC), 4-dimethylamiopyridine (DMAP), N-(tert-butoxycarbonyl)-L-phenylalanine (Phe-^{N}BOC), trifluoroacetic acid (TFA), trifluoromethane-sulfonic acid (TFMSA), thioanisole were purchased from Aladdin; γ-benzyl-L-glutamate N-carboxyanhydride (NCA-BLG) was supplied by Chengdu Enlai Biological Technology Co., Ltd;

doxorubicin hydrochloride and verapamil hydrochloride were purchased from Dalian Meilun Biotech Co., Ltd. 3-(4,5-Dimethylthiazol-2-yl)-2,5-diphenyltetrazoliumbromide (MTT) was purchased from Sigma-Aldrich (China). RPMI-1640 medium, fetal bovine serum (FBS) and phosphate buffer solution (PBS) were purchased from Gibco BRL (Gaithersberg, MD, USA). MCF-7 and MCF-7/ADR resistant cells were kindly donated by the Department of Pharmacology, School of Pharmacy, Shandong University. All the materials were used as received except that ε-caprolactone was purified by vacuum distillation over CaH_2 (purchased from Aladdin).

2.2 Synthesis of polypeptide-based copolymer $mPEG_{2K}$-PCL_{4K}-PGA_{1K}

The synthesis route of $mPEG_{2K}$-PCL_{4K}-PGA_{1K} is shown in Scheme 1 (The details of chemical synthesis and the determination of molecular weight are described in the ESI.†). The first step was to synthesize $mPEG_{2K}$-PCL_{4K}-OH via ROP of ε-caprolactone using $mPEG_{2K}$ as initiator and stannous octanoate as a catalyst.[29] The OH end-group of mPEG-PCL-OH was then reacted with Phe-^{N}BOC under the catalysis of DCC and DMAP to synthesize $mPEG_{2K}$-PCL_{4K}-Phe-^{N}BOC. To obtain $mPEG_{2K}$-PCL_{4K}-NH_2, the BOC group was removed by the acid hydrolysis of TFA. The NCA-BLG was also reacted with the NH_2 end-group of $mPEG_{2K}$-PCL_{4K}-NH_2 through ROP reaction to form the $mPEG_{2K}$-PCL_{4K}-$PBLG_{1K}$.[23] Finally, the benzyl protecting group was removed and the desired product $mPEG_{2K}$-PCL_{4K}-PGA_{1K} was obtained.

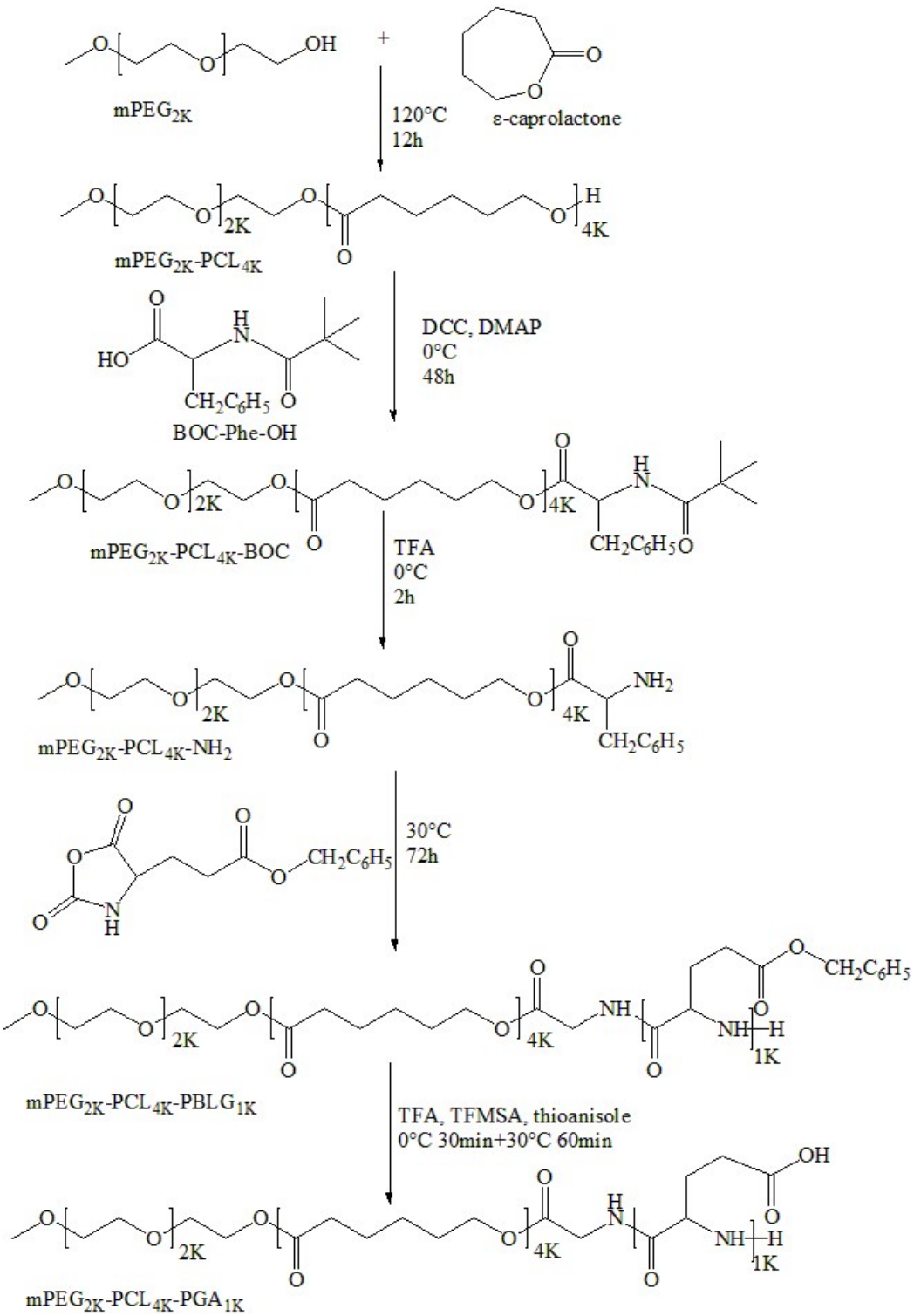

Scheme 1 The synthesis route of $mPEG_{2Kk}$-PCL_{4Kk}-PGA_{1Kk}.

130 2.3 Characterizations of the synthesized $mPEG_{2K}$-PCL_{4K}-PGA_{1K}

131 2.3.1 Nuclear magnetic resonance analysis (^1H NMR)

132 To verify the successful synthesis of copolymers $mPEG_{2K}$-PCL_{4K}-PGA_{1K}, the ^1H
133 NMR spectra of the copolymer (in DMSO-D6) were recorded on a Bruker AV400
134 NMR spectrometer (Bruker, German) at 400MHz.

135 2.3.2 Determination of CAC

136 To determine the critical aggregation concentration (CAC) of the synthesized
137 $mPEG_{2K}$-PCL_{4K}-PGA_{1K}, the fluorescence techniques was applied using pyrene as
138 probe molecules as we have reported previously.[30] Briefly, 40 μL stock pyrene
139 solution (4×10^{-6} mol L^{-1} in ethanol) was transferred to a series of 10 mL tubes. After
140 the ethanol was evaporated, the desired amount of $mPEG_{2K}$-PCL_{4K}-PGA_{1K} solution in
141 water was added to tubes to make the final pyrene concentration be 6×10^{-6} mol L^{-1}
142 and the $mPEG_{2K}$-PCL_{4K}-PGA_{1K} range from 0.001 to 20 mg mL^{-1}. Then all the tubes
143 were equilibrated with ultrasonication for 1 h and stood overnight to make the pyrene
144 molecules solubilize in the aggregates. After setting the excitation wavelength at 334
145 nm, the fluorescence spectra of the samples were recorded from 350 to 450 nm with
146 Hitachi F-7000 fluorescence spectrophotometer and the slit width was set at 2.5 nm
147 for excitation and emission. After calculating the ratio of fluorescence intensities at
148 373 nm (denoted as I_1) and 384nm (denoted as I_3), the CAC was determined using the
149 plot of pyrene I_1/I_3 ratio versus different concentration of copolymers.

150 2.3.3 Morphology of $mPEG_{2K}$-PCL_{4K}-PGA_{1K} in water

151 $MPEG_{2K}$-PCL_{4K}-PGA_{1K} could spontaneously assemble in aqueous solution and
152 the morphology of the aggregates was confirmed by transmission electron microscopy
153 (TEM). Firstly, drops of sample were adsorbed onto the carbon-coated copper grid
154 separately and the redundant sample was removed with filter paper. After dried, the
155 carbon-coated copper grids with samples were observed using a JEOL JEM1400
156 transmission electron microscope.

157 2.4 Preparation of drug-loaded polymersomes

158 The poly(DOX+VER) were prepared via the dialysis method as follows.[31]
159 Briefly, 10 mg $mPEG_{2K}$-PCL_{4K}-PGA_{1K} was dissolved in 0.2 mL DMSO, and then 0.3
160 mL of aqueous solution containing 1.5 mg VER was added dropwise. Because the
161 residual of acids like TFA and TFMSA introduced in the last synthesis step,
162 appropriate amount of NaOH (1 M) was added to tune the pH of the solution to be
163 neutral. After this, 0.3 mL of water solution containing 1 mg DOX was added and the
164 solution was sonicated for about 1 min to accelerate the entrapment of drugs. Finally,
165 the poly(DOX+VER) was dialysed against deionized water (400 mL) in a dialysis bag
166 with a molecular weight cut-off of 3500 Da for 4 h to remove the free drugs, and the
167 deionized water was changed once. Therefore, there is nearly no DMSO molecules
168 existed in the sample.

For preparing DOX-loaded polymersomes (denoted as polyDOX), the procedures were similar with poly(DOX+VER) preparation except that the VER water solution was replaced by water.

The loading capacity of polymersomes was determined by measuring the amount of DOX and VER in poly(DOX+VER) using high performance liquid chromatography (HPLC). The poly(DOX+VER) was destroyed by DMSO and diluted by mobile phase, and then the sample was filtered through a 0.45 μm filter and eluted through a Phenomenex gemini C_{18} column (5 μm，250 mm×4.6 mm, USA). The conditions for HPLC analysis of DOX is listed below: the detection wavelength was set at 266 nm, the mobile phase consists of methanol: 0.01M $NH_4H_2PO_4$: acetic acid (65：35：0.2, *v*/*v*/*v*) and the flow rate was set as 0.7 mL min^{-1}. As for the other drug VER, the detection wavelength was set at 278 nm, the mobile phase consisting of acetic acid-acetic natrium: methanol: three-ethylamine (45：55：1, *v*/*v*/*v*) was delivered at a flow rate of 0.8 mL min^{-1}. Concentration was determined from the calibration curve of drugs in the mixture of DMSO and mobile phase. Drug-loading efficiency (DL) and encapsulation efficiency (EE) were calculated as following:

$$\mathrm{DL}\,\% = \frac{\text{weight of the drugs in polymersomes}}{\text{weight of the copolymer and drugs in polymersomes}} \times 100\,\%$$

$$\mathrm{EE}\,\% = \frac{\text{weight of the drugs in polymersomes}}{\text{weight of the feeding drugs}} \times 100\,\%$$

In order to get high EE and DL for both drugs, various amounts of drugs have been encapsulated into 10 mg $mPEG_{2K}$-PCL_{4K}-PGA_{1K} (Table S1, ESI†). The results

showed that when the ratio of drugs and copolymer was 1:1.5:10 (DOX: VER: $mPEG_{2K}$-PCL_{4K}-PGA_{1K}), the average DL and EE of the two drugs was high. At the selected ratio, the DL and EE of DOX was (5.05±0.26)% and (59.89±3.40)% while that of VER was (10.72±1.08)% and (84.82±9.53)%, respectively.

2.5 Size and size distribution of drug-loaded polymersomes

Dynamic light scattering (DLS) was carried out to determine the size and size distribution of drug-loaded polymersomes using BIC-Brook-Haven (USA) with angle detection at 90°. Before the measurements, all the samples including polyDOX and poly(DOX+VER) were filtered through a 0.45 μm membrane filter to prepare the dust-free solutions.

2.6 Drug release *in vitro*

To verify the sustained and pH-sensitive release of drugs from drug-loaded polymersomes, polyDOX and poly(DOX+VER) which containing the same content of drug were incubated in the dialysis membrane bag with molecular weight cut off of 3500 Da, respectively. Then the dialysis membrane bags were immersed in 20 mL of 0.01M PBS buffers (pH 7.4 and 5.0) at 37 °C with continuously stirring at 100 rpm. At the designated time intervals, 0.5 mL of the samples was withdrawn from the release medium and the same amount of fresh release medium was added immediately. For comparison, the release profile of free drugs DOX and VER were also tested in pH 7.4 and 5.0 PBS. The release solution was filtered through a 0.45 μm membrane

filter which was then used to measure the amount of released DOX and VER by HPLC. The concentration was determined from the calibration curve of DOX and VER in PBS (pH 7.4 and 5, respectively) and the cumulative amount of drugs was calculated with the following equation:

$$\text{Cumulative amount released}\,\% = \frac{M_t}{M_{total}} \times 100\,\%$$

M_t refers to the amount of the released drug from drug-loaded polymersomes at time t and M_{total} refers to the total amount of drugs loaded in drug-loaded polymersomes.

2.7 Cytotoxicity assay *in vitro*

The *in vitro* cytotoxicity of free DOX, polyDOX and poly(DOX+VER) to MCF-7 and MCF-7/ADR resistant cells were determined by MTT method.[32] Briefly, MCF-7 and MCF-7/ADR resistant cells were transferred to 96-well tissue culture plates at a seeding density of 5000 cells per well (0.1 mL medium). Following by attachment overnight, the culture medium in each well was carefully replaced with medium containing serial dilutions of treatment drugs including free DOX, polyDOX and poly(DOX+VER). The concentrations of DOX were ranging from 0.01 μg mL^{-1} to 20 μg mL^{-1} (0.01 μg mL^{-1}, 0.1 μg mL^{-1}, 1 μg mL^{-1}, 10 μg mL^{-1} and 20 μg mL^{-1}). At scheduled time intervals (24 h, 48 h and 72 h), 10 μL of 5 mg mL^{-1} MTT dissolved in PBS was added to each well and the plates were incubated for 4 h at 37 °C. After removing the medium, 150 μL of DMSO was added to each well to dissolve the

formed purple crystals derived from MTT with vigorously stirring the plates. The absorbance of each well was read on a microplate reader (Enspire instruments, Perkin Elmer, America) at a wavelength of 490 nm.

In the study, untreated cells served as control and were taken as 100% viability and all the samples were performed in triplicate to give the average and standard deviation (SD). Based on the absorbance of each well, the percentage of cell growth inhibition was calculated as follows: inhibitory rate = $(A_{control}\text{-}A_{sample})/(A_{control}\text{–}A_{blank})\times 100\%$. $A_{control}$ and A_{blank} referred to the absorbance of the culture medium in the presence and absence of cells; A_{sample} referred to the absorbance of the cells respectively treated with free DOX, polyDOX and poly(DOX+VER).

2.8 Cellular uptake and flow cytometric analysis

The cellular uptake of free DOX and drug-loaded polymersomes including polyDOX and poly(DOX+VER) was tested using inverted fluorescence microscope. Since DOX showed the red color and could act as a fluorescent probe, all the samples were tested directly without using another fluorescence molecule.[33] MCF-7 and MCF-7/ADR resistant cells were seeded into 6-well culture plates at a density of 2×10^5 cells per well and incubated overnight. The cells were then respectively treated with free DOX, polyDOX or poly(DOX+VER) at a final DOX concentration of 3 μg mL^{-1} and allowed to be incubated for 2 h. After washed three times with PBS, all the samples were imaged using inverted fluorescence microscope.

To determine the cellular uptake of free DOX, polyDOX or poly(DOX+VER) quantitatively, the fluorescence intensity in the cells treated with different samples was tested using flow cytometry. The cells treated as described above were also seeded into 6-well culture plates at a density of 2×10^5 cells per well and incubated overnight. After being incubated for 2 h and harvested by trypsinization with centrifugation, the cells were suspended in 200 μL of PBS. Finally, the fluorescence intensity in the cells was determined using a flow cytometer. The number of cells collected was ten thousand, and the experiments were run in triplicate.

2.9 Hemolysis test

The hemoglobin released from rabbit blood was used to evaluate the hemolytic activities of blank polymersomes by spectrophotometry. Whole rabbit blood samples were centrifugated and resuspended in normal saline to get the red blood cells (RBCs 2%). 1.25 mL RBCs suspension mixed with 1.25 mL normal saline solution and 1.25 mL distilled water were served as negative control (producing no hemolysis) and positive control (producing 100% hemolysis), respectively. 0.15 mL of blank polymersomes solution with different concentration (0.014 mg mL^{-1}, 0.07 mg mL^{-1}, 0.14 mg mL^{-1}, 0.7 mg mL^{-1} and 1.4 mg mL^{-1}) were added into the mixture of 1.25 mL RBCs suspension and 1.1 mL normal saline solution. After kept at (37.0±1.0) °C for 3 h, all the samples were centrifuged at 1500 rpm for 15 minutes. The absorbance of supernatants was measured with UV spectrophotometer at 540 nm and the normal saline was used as blank.

The hemolysis ratio of RBSs was calculated using the following formula: Hemolysis (%) = $(A_{sample}-A_{negative})/(A_{positive}-A_{negative})\times 100\%$, where A_{sample}, $A_{negative}$, $A_{positive}$ refer to the absorption of blank polymersomes, negative control and positive control at 540 nm, respectively.

3. Results and discussion

3.1 Characterization of the synthesized $mPEG_{2K}$-PCL_{4K}-PGA_{1K}

3.1.1 Nuclear magnetic resonance analysis (^{1}H NMR)

The characterization of $mPEG_{2K}$-PCL_{4K}-PGA_{1K} was shown in Fig.1. The location of the peaks and assignment of the letters shown in ^{1}H NMR spectra were listed as below: ***mPEG***: a (δ 3.32) C**H$_3$**OCH$_2$CH$_2$O, b (δ 3.51) CH$_3$O**CH$_2$CH$_2$**O; ***PCL***: c (δ 2.26) COC**H$_2$**CH$_2$CH$_2$CH$_2$CH$_2$O, d (δ 1.54) COCH$_2$C**H$_2$**CH$_2$C**H$_2$**CH$_2$O, e (δ 1.29) COCH$_2$CH$_2$C**H$_2$**CH$_2$CH$_2$O, f (δ 3.97) COCH$_2$CH$_2$CH$_2$CH$_2$C**H$_2$**O; ***BOC-Phe-OH***: g (δ 7.26) COCH(CH$_2$C$_6$**H$_5$**)NH; ***PBLG***: g (δ 7.26)COCH(CH$_2$CH$_2$COOCH$_2$C$_6$**H$_5$**)NH, h (δ 5.06) COCH(CH$_2$CH$_2$COOC**H$_2$**C$_6$H$_5$)NH.

The Fig. 1A was the spectrum of $mPEG_{2K}$-PCL_{4K}-OH. Based on the comparison of the peak areas at 3.51 ppm (b) and 2.26 ppm (c),[34] the molecular weight of PCL was estimated to be 4K. Due to the fact that the peak of COC(C**H$_3$**)$_3$ in BOC-Phe-OH was overlapped with the peak of H labeled with "e" in the PCL block at 1.29 ppm, the ratio of peak at 1.54 ppm (d) and 1.29 ppm (e) decreased from 2:1 to 1.59:1 confirmed

the successful conjugation of BOC-Phe-OH which was also proved by the appearance of the peak at 7.26 ppm (g).[35] After removing the BOC group to get $mPEG_{2K}$-PCL_{4K}-NH_2 by acidolysis, the ratio of the peak at 1.54 ppm (d) and 1.29 ppm (e) got back to 2:1. To back up the successful synthesis of $mPEG_{2K}$-PCL_{4K}-$PBLG_{1K}$, the representative peak of $COCH(CH_2CH_2COOC\mathbf{H_2}C_6H_5)NH$ was show at 5.06 ppm (h). Based on the comparison of the peak areas at 5.06 ppm (h) and 2.26 ppm (c), the molecular weight of PBLG was estimated to be 1K. In the last step, the disappearance of the peak at 5.06 ppm (h) confirmed that the benzyl group of PBLG was removed and the target product $mPEG_{2K}$-PCL_{4K}-PGA_{1K} was synthesized successfully.

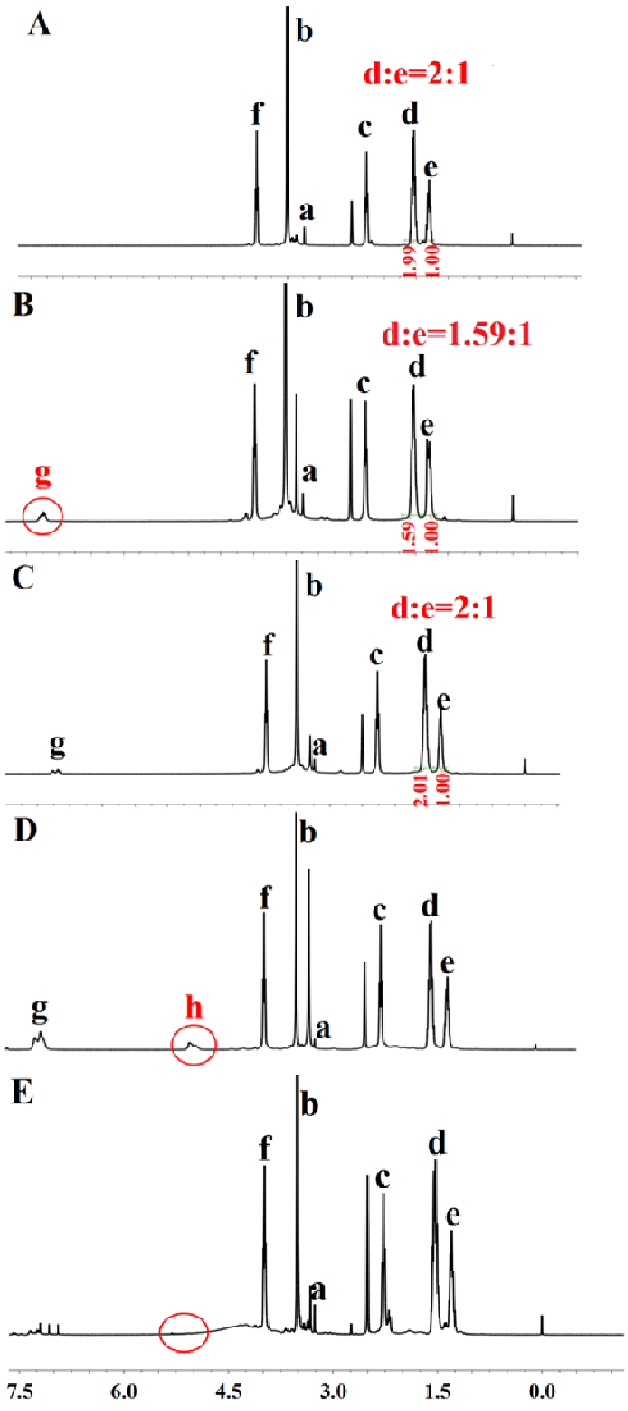

298

299 Fig.1 The ^{1}H NMR spectra of (A) $mPEG_{2K}$-PCL_{4K}-OH (B) $mPEG_{2K}$-PCL_{4K}-BOC (C)

300 $mPEG_{2K}$-PCL_{4K}-NH_2 (D) $mPEG_{2K}$-PCL_{4K}-$PBLG_{1K}$ (E) $mPEG_{2K}$-PCL_{4K}-PGA_{1K} in

301 DMSO-D6.

3.1.2 Determination of CAC

Pyrene was the most widely used fluorescent molecule for determining the CAC and its fluorescence spectrum was shown Fig. S1 (ESI†). The I_1/I_3 ration of pyrene emission spectra was related with the polarity where the pyrene located.[36] The I_1/I_3 ratio of fluorescence emission spectra of pyrene versus concentration of $mPEG_{2K}$-PCL_{4K}-PGA_{1K} was shown in Fig. 2. It could be seen that at the beginning I_1/I_3 ratio slightly decreased and then abruptly decreased with the increase of copolymer concentration. From the break point the CAC of the copolymer could be determined about 0.0776 mg mL^{-1} (1.1086×10^{-5} mol L^{-1}). At the beginning, the pyrene molecules was in the polar environment (water), with the polymer concentration increasing, there was aggregates formed in the solution and the pyrene could be solubilized in the hydrophobic domain of the aggregates, leading to the decrease of I_1/I_3 ratio. The low CAC of $mPEG_{2K}$-PCL_{4K}-PGA_{1K} guarantee the stability of the polymersomes diluted in the vivo.

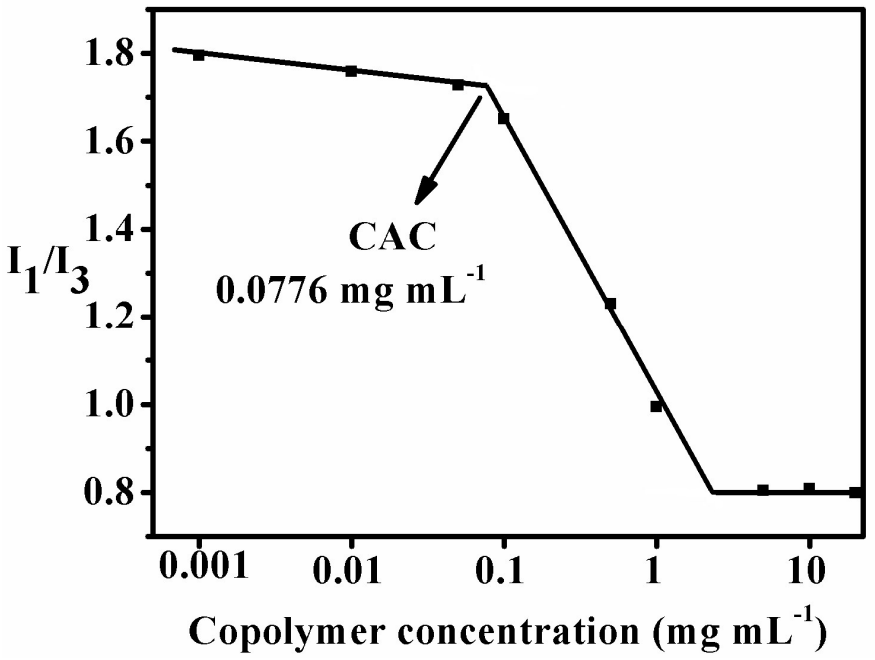

316

317 Fig. 2 The I_1/I_3 ratio of fluorescence emission spectra of pyrene versus concentration

318 of $mPEG_{2K}$-PCL_{4K}-PGA_{1K}.

319 3.1.3 Morphology of $mPEG_{2K}$-PCL_{4K}-PGA_{1K} in water

320 The copolymer $mPEG_{2K}$-PCL_{4K}-PGA_{1K} could self-assemble in water and the

321 solution was blue-opalescent (Fig. 3A) and the morphology of the aggregates was

322 examined by TEM images (Fig. 3B, Fig. S2 in ESI†). It could be seen that the

323 uniform spherical aggregates with the diameter about 50-60 nm were formed in the

324 solution. From Fig. 3B and Fig. S2 it could be clearly seen that the polymer assembly

325 were hollow spheres containing an aqueous solution in the core surrounded by a

326 bilayered membrane. A characteristic dark rim on the outer surface was an obvious

327 indication of the hollow morphology of polymersomes. [37] Therefore, they could be

applied to deliver hydrophilic drugs efficiently. The appropriate size of polymersomes facilitates the EPR effect for passive targeting for the tumor issue.

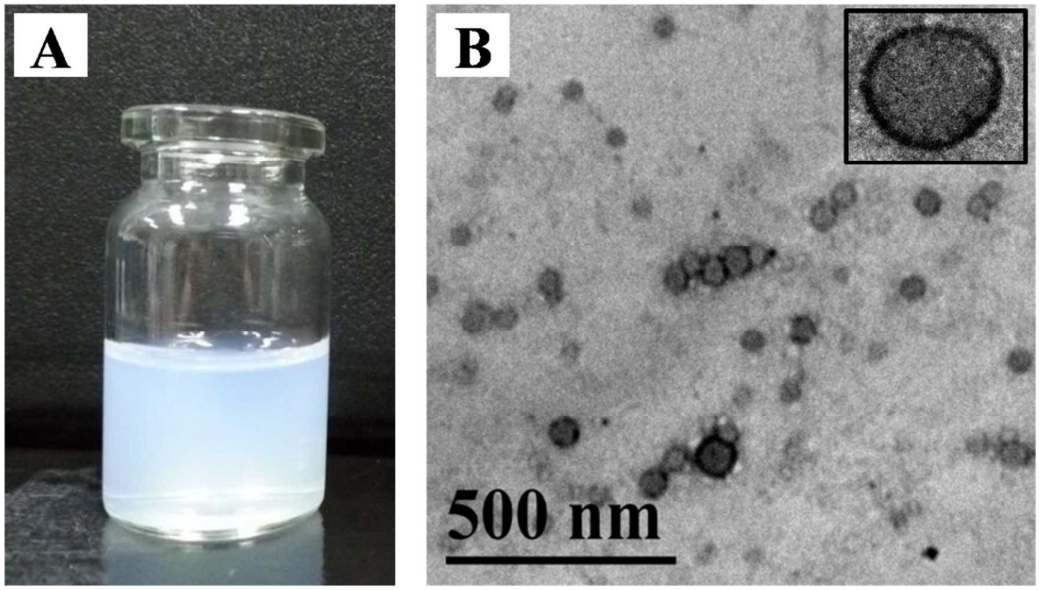

Fig. 3 (A) Photograph of $mPEG_{2K}$-PCL_{4K}-PGA_{1K} aqueous solution. (B) Morphology of $mPEG_{2K}$-PCL_{4K}-PGA_{1K} self-assembly in water. Insert: the TEM blowup of a single polymersome.

3.2 Size and size distribution of drug-loaded polymersomes

The size and size distribution of drug-loaded polymersomes were characterized by DLS. As shown in Fig. 4, both polyDOX and poly(DOX+VER) showed a unimodal and narrow size distribution (PDI: 0.04-0.09), and the diameter were (58.8±0.3) nm and (44.9±0.5) nm, respectively. The size of the drug-loaded polymersomes was appropriate for EPR effect to achieve passive targeting.

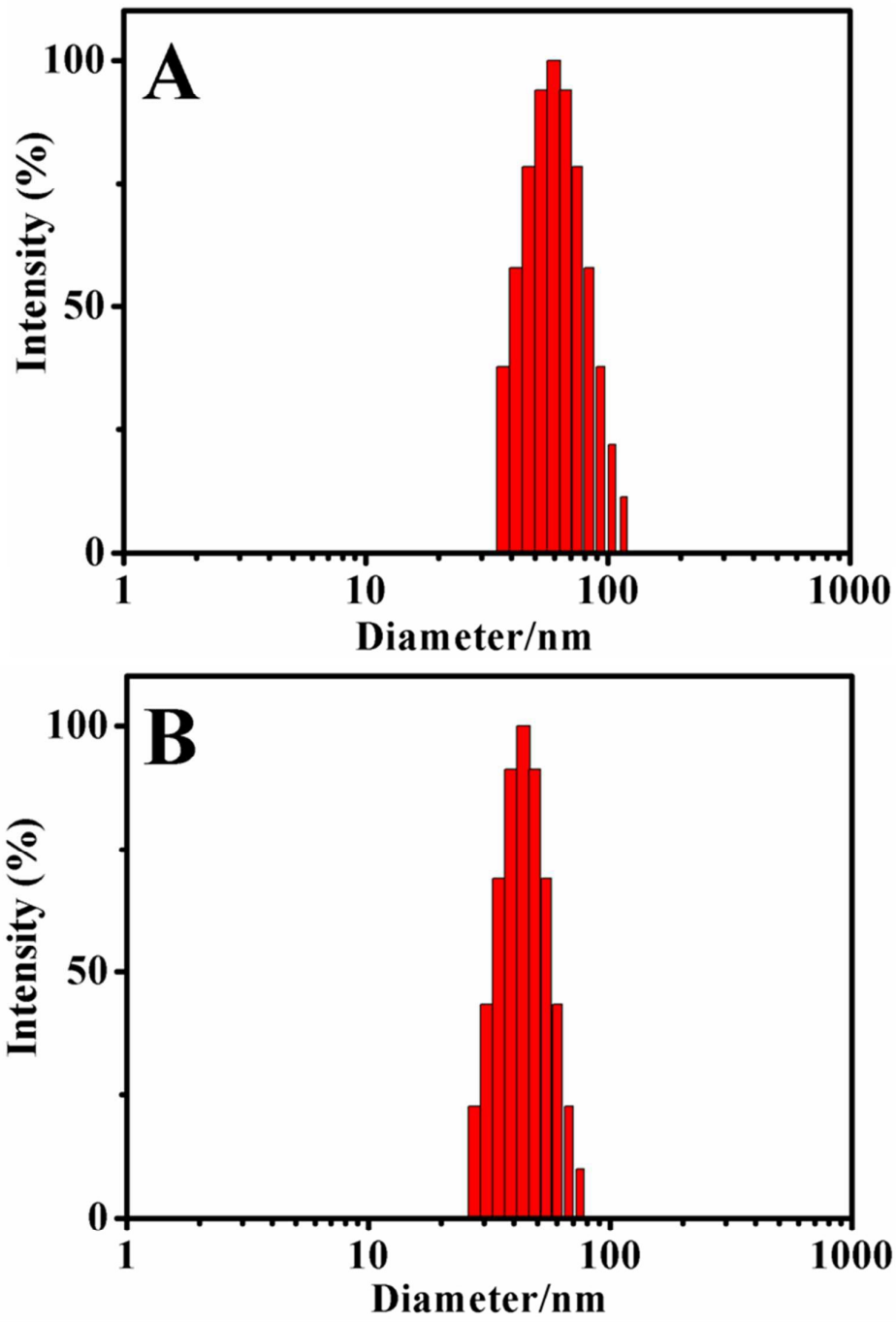

341

342 Fig. 4 The size and size distribution of drug-loaded polymersomes (A) polyDOX and

343 (B) poly(DOX+VER).

344

345 3.3 Drug release *in vitro*

346 The drug release profiles in PBS with different pH value were shown in Fig. 5. It
347 could be seen from Fig. 5A that firstly the release of DOX from polyDOX and
348 poly(DOX+VER) was more sustained than that from the free DOX solution. For
349 example, free DOX released almost completely in 24 h while polyDOX and
350 poly(DOX+VER) only released 19.03% and 18.94% in pH 7.4 PBS. Secondly, the
351 addition of VER has no effect on the release of DOX from the polymersomes, which
352 was proved by the almost same release plots for the polyDOX and poly(DOX+VER)
353 in pH 7.4 and pH 5.0 PBS. Thirdly, the drug-loaded polymersomes showed the
354 pH-sensitive release behavior and the release of DOX from polyDOX and
355 poly(DOX+VER) was higher in pH 5.0 PBS than that in pH 7.4 PBS. Though the low
356 pH could facilitate the solubility and accelerate the release of DOX，the faster release
357 rate of DOX from polyDOX and poly(DOX+VER) at pH 5.0 than that at 7.4 was
358 mainly due to the structure breakage of the polypeptide-based polymersomes in acid
359 environment. Conclusively, the prepared polymersomes showed good pH-sensitive
360 property and the obvious sustained release behaviour, which was desirable for the
361 efficient cancer therapy.

362 Fig. 5B showed VER release behaviour from the poly(DOX+VER). Similarly,
363 VER also showed a sustained and pH-sensitive release from poly(DOX+VER). The
364 released VER amounts were about 91.74% and 71.63% from the poly(DOX+VER) in
365 pH 5.0 and pH 7.4 PBS after 24 h, respectively. The sustained-release time of VER

366 from poly(DOX+VER) was not as long as that of DOX was mostly due to the strong
367 electrostatic interactions between DOX and PGA.[38]

368 Based on the above results, the copolymer $mPEG_{2K}$-PCL_{4K}-PGA_{1K} could act as a
369 promising drug carrier with high pH-sensitive property. Thus the drug-loaded
370 polymersomes could accelerate the drug release and improve the accumulation of
371 drugs in acidic tumor issue to enhance the anti-cancer effect. In addition, the sustained
372 release of drugs from the polymersomes could make the drug constantly fight against
373 cancer cells inducing the increased cancer cells inhibition.

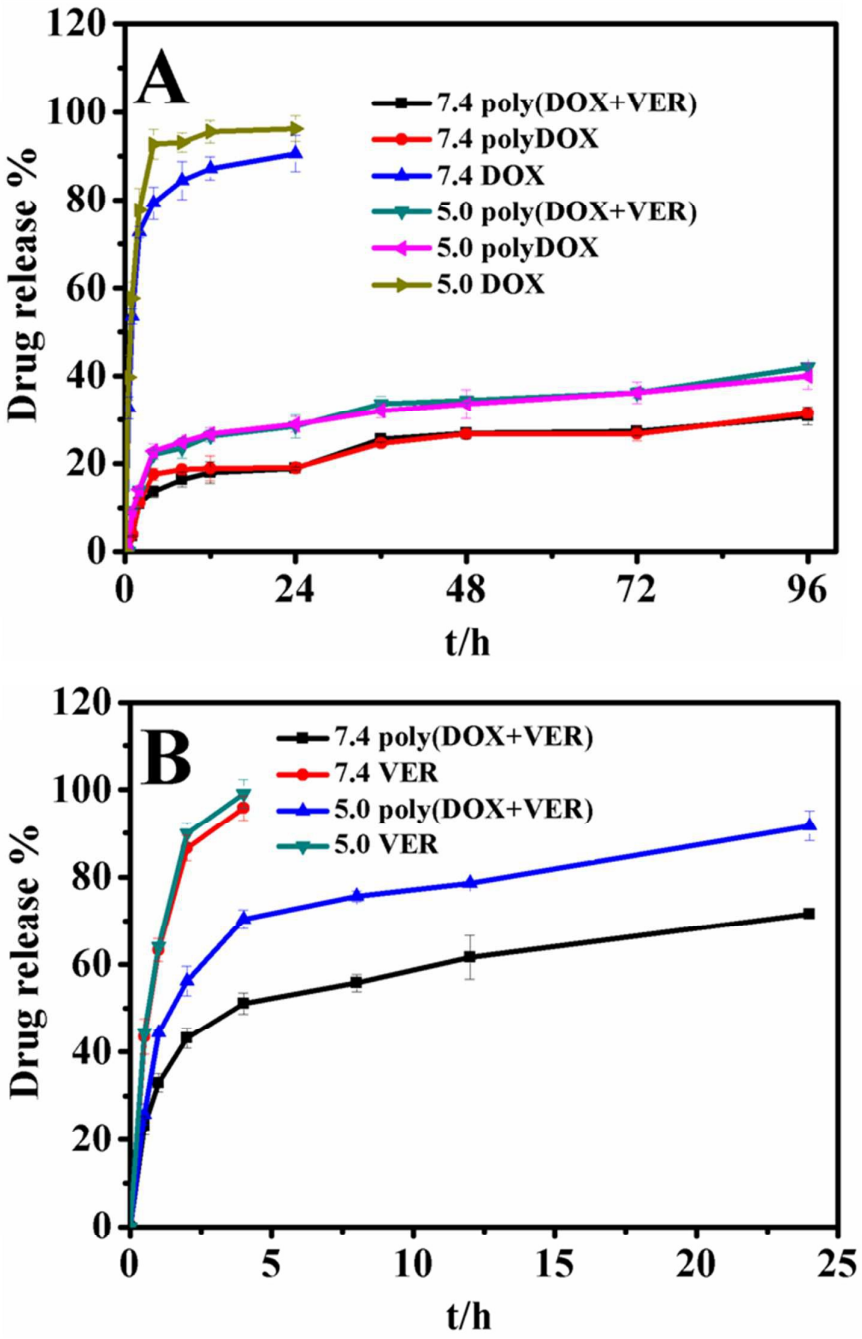

374

375 Fig. 5 The *in vitro* release profiles of (A) DOX and (B) VER from polymersomes in

376 different PBS (pH 7.4 and 5.0). The release profiles of free DOX and VER solutions

377 were investigated as control. Data as mean ± SD, n=3.

3.4 Cytotoxicity assay *in vitro*

To verify the antitumor effect of the drug-loaded polymersomes, the cell inhibition of the blank polymersomes was tested with the concentration of copolymer ranging from 0.1 to 500 μg mL^{-1}. The blank polymersomes had no apparent cytotoxicity on cancer cells as shown in Fig. S3 (ESI†). The *in vitro* antitumor activity of drug-loaded polymersomes was tested and that of free DOX was used as control. As illustrated in Fig. 6, the inhibition rate of the samples increased with an increasing drug concentration from 0.01 μg mL^{-1} to 20 μg mL^{-1} for both MCF-7 and MCF-7/ADR cells. For the MCF-7 cells, free DOX sample showed a little higher inhibition ratio than that of polyDOX or poly (DOX+VER) sample due to the incomplete release of DOX from drug-loaded polymersomes which was confirmed from Fig. 5A. The polyDOX and poly(DOX+VER) exhibited similar inhibition ratio, which indicated that the VER had almost no cytotoxicity to cancer cells.[39] However, for the MCF-7/ADR cells, the inhibitory effect of poly(DOX+VER) was much stronger than that of free DOX or polyDOX especially at 48 h and 72 h, indicating that the addition of p-gp inhibitor VER could significantly improve the cytotoxicity of DOX to cancer resistant cells.

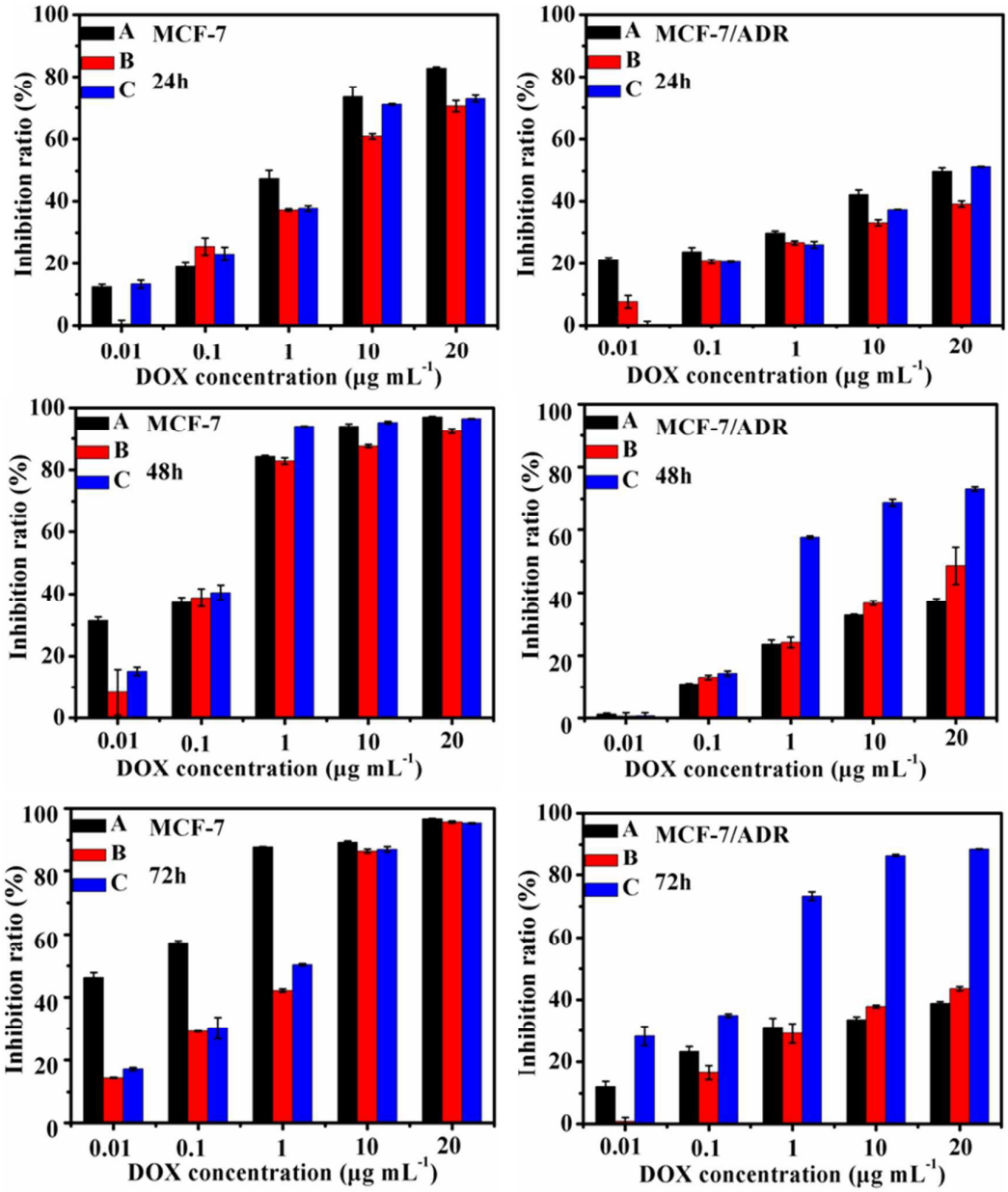

Fig. 6 The inhibition ratio to MCF-7 and MCF-7/ADR cells incubated with different samples (A) DOX (B) polyDOX and (C) poly(DOX+VER).

In order to further confirm the enhanced cytotoxicity and resistant ability of poly(DOX+VER) against MCF-7/ADR cells, the IC_{50} value and resistance reversion index (RRI) were calculated and listed in Table 1. The IC_{50} values of

poly(DOX+VER) were 10.14±3.02 μg ml^{-1}, 2.71±0.35 μg ml^{-1} and 0.15±0.02 μg ml^{-1} respectively at 24, 48 and 72 h, much lower than that of free DOX (55.46±3.73 μg ml^{-1} for 24 h, 31.85±6.82 μg ml^{-1} for 48 h and 7.32±0.94 μg ml^{-1} for 72 h). The difference in IC_{50} values indicated that poly(DOX+VER) has a much higher cytotoxicity in MCF-7/ADR cells than free DOX. RRI was an important parameter for evaluating the reversal activity of MDR reversal agents. At 24 h, 48 h and 72 h, the RRIs of poly(DOX+VER) were 5.47, 11.75 and 48.8, respectively, indicating the poly(DOX+VER) could reverse the resistance of MCF-7/ADR cells to DOX in 72 h successfully. Therefore, the poly(DOX+VER) had high ability to inhibit the proliferation of MCF-7/ADR cells.

Table 1 IC_{50} (mean±SD, n=3) and RRI of poly(DOX+VER) against MCF-7/ADR cells.

	IC_{50} (μgml^{-1})			RRI		
	24h	48h	72h	24h	48h	72h
DOX	55.46±3.73	31.85±6.82	7.32±0.94	-	-	-
Poly(DOX+VER)	10.14±3.02	2.71±0.35	0.15±0.02	5.47	11.75	48.8

RRI = IC_{50}(free DOX)/IC_{50}(poly(DOX+VER)).

3.5 Cellular uptake studies and flow cytometric analysis

The cellular uptake of free DOX, polyDOX and poly(DOX+VER) on MCF-7 and MCF-7/ADR cells were visualized quantitatively by inverted fluorescence

418 microscope. As illustrated in Fig. 7, detectable DOX red fluorescence was present in
419 these cancer cells. It could be seen that the red fluorescence intensity of free DOX,
420 polyDOX and poly(DOX+VER) on MCF-7 cells almost showed no difference. This is
421 because that the free DOX could readily diffuse across the cell membrane to induce
422 high cellular uptake.[40] Since DOX could be easily pumped out by P-gp in
423 MCF-7/ADR cells membranes,[41] an obvious disparity in red fluorescence intensity of
424 free DOX, polyDOX and poly(DOX+VER) has been revealed on MCF-7/ADR cells:
425 the red fluorescence intensity of poly(DOX+VER) was higher than that of polyDOX
426 or free DOX. All these indicated that $mPEG_{2K}$-PCL_{4K}-PGA_{1K} could deliver drugs into
427 cancer cells successfully, and poly(DOX+VER) could inhibit the expression of P-gp
428 and improve the accumulation of DOX in MCF-7/ADR cells significantly.

429

430

431

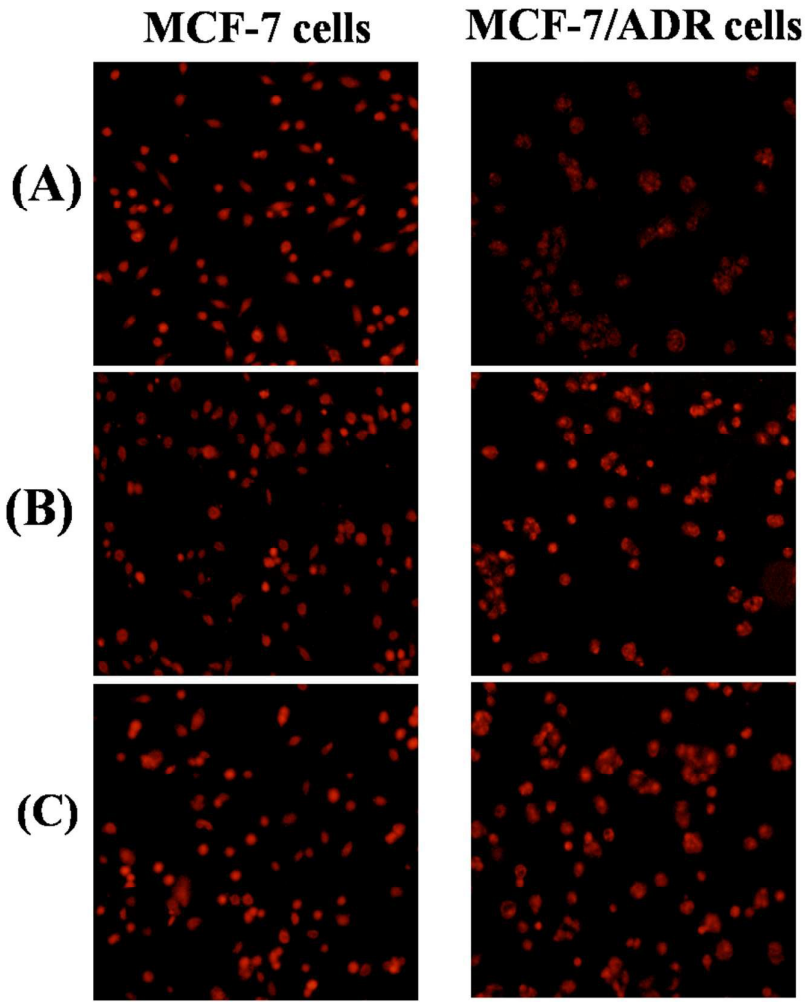

Fig. 7 Fluorescence microscopy images of MCF-7 cells and MCF-7/ADR cells, after incubation for 2 h treated with (A) DOX, (B) polyDOX and (C) poly(DOX+VER) with an equivalent DOX concentration of 3 μg mL^{-1}.

Fig. 8 quantitatively supports the results mentioned above by flow cytometry on MCF-7 and MCF-7/ADR cells incubated in free DOX, polyDOX and poly(DOX+VER). The untreated cells served as the control. For the MCF-7 cells, the intracellular fluorescence intensity of free DOX, polyDOX and poly(DOX+VER) was

similar. However, the intracellular fluorescence intensity of poly(DOX+VER) was stronger than that of free DOX for MCF-7/ADR cells because the significant decrease in pumpout of free DOX and the different mechanism to enter cells.[42] In addition, the intracellular fluorescence intensity of poly(DOX+VER) was also higher than that of polyDOX, indicating that the addition of VER could inhibit the expression of P-gp to reduce the pumpout of DOX significantly. In a word, the poly(DOX+VER) entered into cells via endocytosis mechanism could decrease the pumpout and increase the accumulation of DOX in cancer cells especially resistant cancer cell successfully.

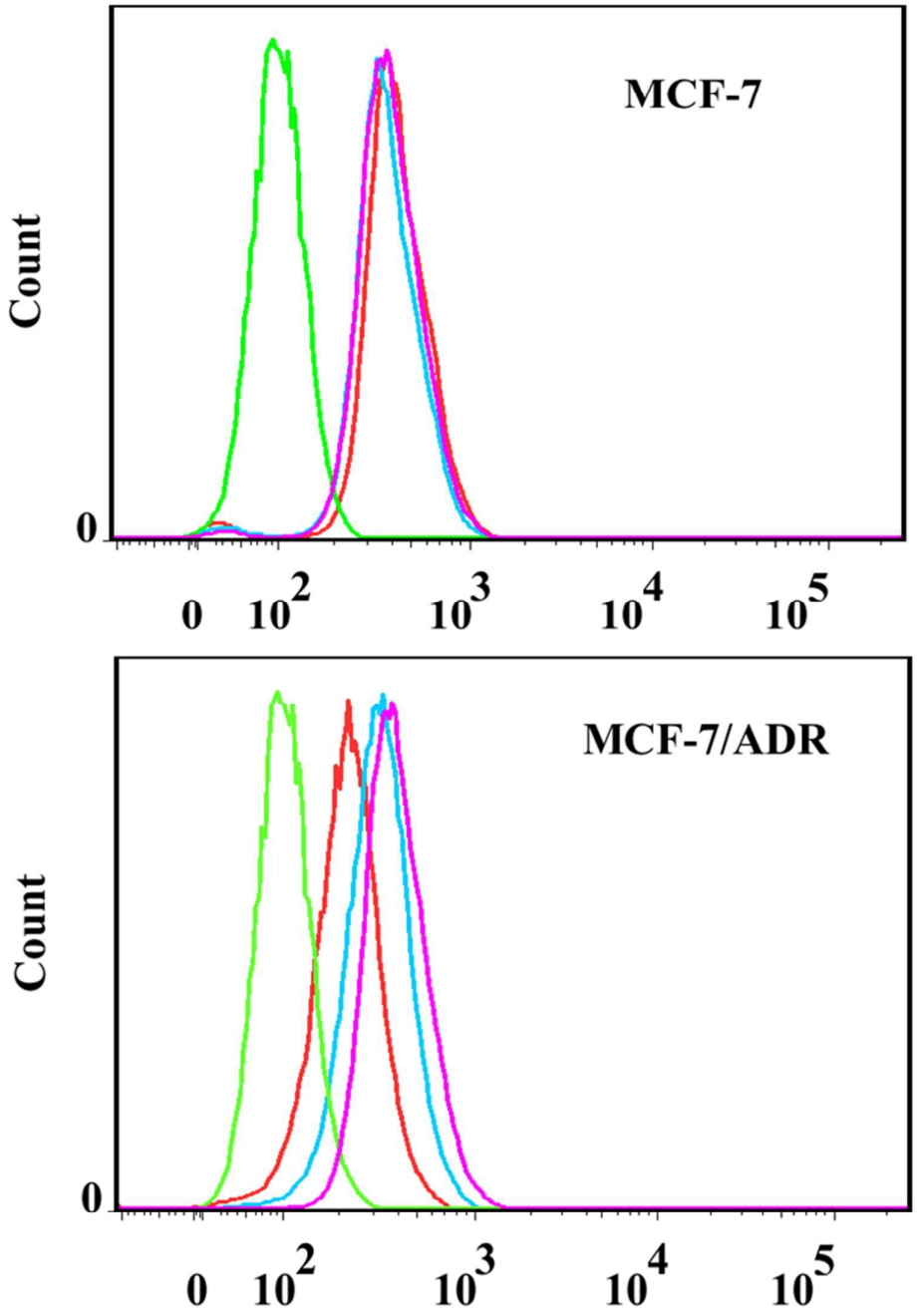

449

450 Fig. 8 Fluorescence intensity of MCF-7 and MCF-7/ADR cells analyzed by flow

451 cytometry after treatment with different formulations with an equivalent DOX of 3μg

452 mL^{-1} for 2 h. Control (green), DOX (red), polyDOX (blue), poly(DOX+VER) (pink).

453 3.6 Hemolysis test

Hemolysis, defined as the release of hemoglobin into plasma due to damage of erythrocytes membrane, was the important index to evaluate the blood compatibility of copolymers. This is because that most of copolymers were designed to be administrated via intravenous injection for the drug delivery applications.[43] The hemolisis ratio was usually tested by the UV absorbance of hemoglobin and it has been reported that the pharmaceutical preparation could be applied for intravenous injection when the hemolysis ratio was under 10%.[44] Fig. 9 exhibited the hemolysis ratio of copolymer $mPEG_{2K}$-PCL_{4K}-PGA_{1K} with different concentration. At all concentration of copolymer from 0.014 to 1.4 mg mL^{-1}, the hemolysis ratio was below 5%, indicating the high blood compatibility of the synthesized copolymer $mPEG_{2K}$-PCL_{4K}-PGA_{1K} and it was suitable for intravenous injection.

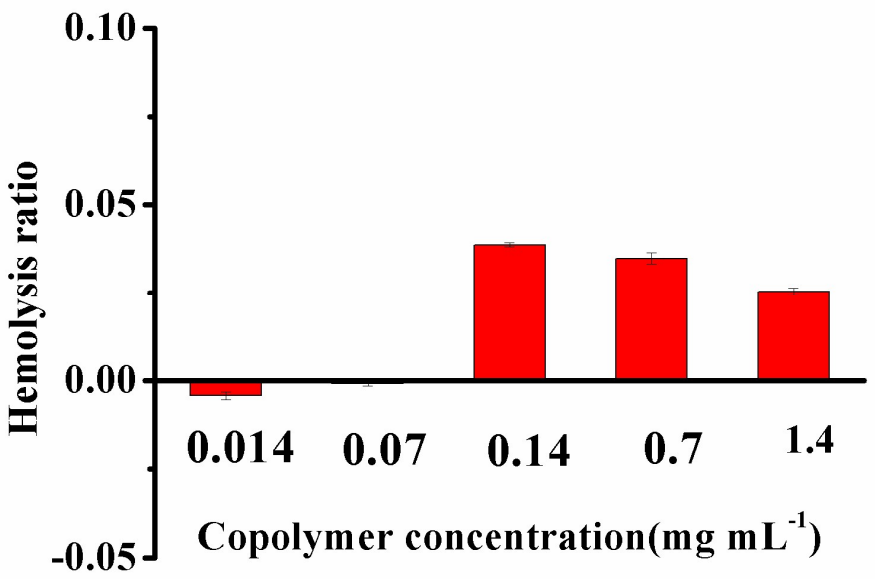

Fig. 9 The hemolysis ratio induced by copolymer $mPEG_{2K}$-PCL_{4K}-PGA_{1K} with different concentration incubated at (37.0±1.0) °C for 3 h.

4. Conclusion

In the present study, a pH-sensitive polypeptide-based block copolymer $mPEG_{2K}$-PCL_{4K}-PGA_{1K} was synthesized and it could self-assemble into polymersomes to co-deliver the hydrophilic drugs DOX and VER. The size of the polymersomes was about 50-60 nm, which was the appropriate size for EPR effect to achieve passive targeting and improve the accumulation of drugs in tumor issue. In addition, the pH-sensitive property of poly(DOX+VER) made the high accumulation of drugs in target site by accelerating the release of drugs at tumor issue (acidic environment) and simultaneously reducing the amount of drugs in the blood circulation. The poly(DOX+VER) showed much higher cytotoxicity and cellular uptake on MCF-7/ADR resistant cells than polyDOX or free DOX. However, there was nearly no differences for the three formulations on MCF-7 cells, suggesting that VER could inhibit the expression of p-gp on resistant cancer cells successfully and improve the anticancer effect of DOX. In addition, the low hemolysis ratio of copolymer to rabbit RBCs indicated that it could be applied safely for intravenous injection. Conclusively, encapsulating both anticancer drug DOX and p-gp inhibitor VER in pH-sensitive polymersomes could markedly increase the tumor growth inhibition ability and reduce the side effects of the drug during the therapeutic procedure. Therefore, the prepared poly(DOX+VER) could effectively reverse the

multidrug resistance and was expected to be a promising drug delivery system for cancer therapy.

Acknowledgements

We gratefully acknowledge the financial support from National Natural Science Foundation of China (NSFC, No. 21373126) and the China–Australia Centre for Health Sciences Research (CACHSR).

References

1 T. Genzou and H. Fujiwara, *Prog. Cardiovasc. Dis.*, 2007, **49**, 330-352.

2 K. K. Upadhy, A. N. Bhatt, A. K. Mishra, B. S. Dwarakanath, S. Jain, C. Schatz, J. F. L. Meins, A. Farooque, G. Chandraiah, A. K. Jain, A. Misra and S. Lecommandoux, *Biomaterials*, 2010, **31**, 2882-2892.

3 G. Szakács, J. K. Paterson, J. A. Ludwig, C. Booth Genthe and M. M. Gottesman.. *Nat. Rev. Drug Discov.*, 2006, **5**, 219-234.

4 A. Abolhoda, A. E. Wilson, H. Ross, P. V. Danenberg, M. Burt and K. W. Scotto. *Clin. Cancer Res.*, 1999, **5**, 3352-3356.

5 Y. J. Gu, J. Cheng, C. W.-Y. Man, W. T. Wong and S. H. Cheng, *Nanomed. Nanotechnol. Biol. Med.*, 2012, **8**, 204-211.

6 G. Speelmans, R. W. H. M. Staffhorst, F. A. De Wolf and B. De Kruijff, *Biochim.*

Biophys. Acta., 1995, **1238**, 137-146.

7 A. Singh, M. Talekar, T. H. Tran, A. Samanta, R. Sundaram and M. Amiji, *J. Mater. Chem. B*, 2014, **2**, 8069–8084

8 J. C. Wang, X. Y. Liu, W. L. Lu, A. Chang, Q. Zhang, B. C. Goh and H. S. Lee, *Eur. J. Pharm. Biopharm.*, 2006, **62**, 44-51.

9 L. Candussio, G. Decorti, E. Crivellato, M. Granzotto, A. Rosati, T. Giraldi and F. Bartoli, *Life sci.*, 2002, **71**, 3109-3119.

10 M. Qin, Y. E. K. Lee, A. Ray and R. Kopelman, *Macromol. Biosci.*, 2014, **14**, 1106–1115.

11 F. Meng and Z. Zhong, *J. Phys. Chem. Lett.*, 2011, **2**, 1533-1539.

12 J. Wu, Y. Lu, A. Lee, X. Pan, X. Yang, X. Zhao and R. J. Lee, *J. Pharm. Pharm. Sci.*, 2007, **10**, 350-357

13 J. M. Shen, F. Y. Gao, T. Yin, H. X. Zhang, M. Ma, Y. J. Yang and F. Yue, *Pharmacol. Res.*, 2013, **70**, 102-115.

14 B. Chen, C. Wu, R. X. Zhuo and S. X. Cheng, *RSC Adv.*, 2015, **5**, 6807–6814.

15 Y. C. Huang, Y. S. Yang, T. Y. Lai and J. S. Jan. *Polymer*, 2012, **53**, 913-922.

16 J. Gaspard, J. A. Silas, D. F. Shantz and J. S. Jan, *Supramol. Chem.*, 2010, **22**, 178-185.

17 M. T. Popescu, M. Korogiannaki, K. Marikou and C. Tsitsilianis, *Polymer*, 2014, **55**, 2943-2951.

18 H. Oliveira, E. Pérez Andrés, J. Thevenot, O. Sandre, E. Berra and S.

Lecommandoux, *J. Control. Release*, 2013, **169**, 165-170.

19 H. Yin, H. C. Kang, K. M. Hu and Y. H. Bae, *Colloids Surf. B*, 2014, **116**, 128-137.

20 P. Ni, Q. Ding, M. Fan, J. Liao, Z. Qia, J. Luo, X. Li, F. Luo, Z. Yang and Y. Wei, *Biomaterials*, 2014, **35**, 236-248.

21 T. K. Endres, M. Beck Broichsitter, O. Samsonova, T. Renette and T. H. Kissel, *Biomaterials*, 2011, **32**, 7721-7731.

22 G. Gu, H. Xia, Q. Hu, Z. Liu, M. Jiang, T. Kang, D. Miao, Y. Tu, Z. Pang, Q. Song, L. Yao, H. Chen, X. Ga and J. Chen, *Biomaterials*, 2013, **34**, 196-208.

23 J. Huang and A. Heise, *Chem. Soc. Rev.*, 2013, **42**, 7373-7390.

24 R. H. Juan and S. Lecommandoux, *J. Am. Chem. Soc.*, 2005, **127**, 2026-2027.

25 W. Li, F. Nicol and F. C. Szoka. *Adv. Drug Delivery Rev.*, 2004, **56**, 967-985.

26 H. Hatakeyama, E. Ito, H. Akita, M. Oishi, Y. Nagasaki, S. Futaki and H. Harashima, *J. Control. Release*, 2009, **139**, 127-132.

27 B. F. Lin, D. Missirlis, D. V. Krogstad and M. Tirrell, *Biochemistry*, 2012, **51**, 4658-4668.

28 K. Sano, T. Nakajima, P. L. Choyke and H. Kobayashi, *ACS Nano*, 2012, **7**, 717-724.

29 N. E. Kamber, W. Jeong, S. Gonzalez, J. L. Hedrick and R. M. Waymouth, *Macromolecules*, 2009, **42**, 1634-1639.

30 X. Ji, C. Shi, L. Qi, Y. Guo, N. Li, Z. Li and Y. Luan, *RSC Adv.*, 2014, **4**,

62698-62707.

31 Z. Tian, M. Wang, A. Y. Zhang and Z. G. Feng, *Polymer*, 2008, **49**, 446-454.

32 L. Qi, Y. Guo, J. Luan, D. Zhang, Z. Zhao and Y. Luan, *J. Mater. Chem. B,* 2014, **2**, 8361-8371.

33 X. Yang, H. Hong, J. J. Grailer, I. J. Rowland, A. Javadi, S. A. Hurley, Y. Xiao, Y. Yang, Y. Zhang, R. J. Nickles, W. Cai, D. A. Steeber and S. Gong, *Biomaterials*, 2011, **32**, 4151-4160.

34 W. Zhu, Y. Li, L. Liu, Y. Chen and F. Xi, *Int. J. Pharm.*, 2012, **437**, 11-19.

35 P. Liu, H. Yu, Y. Sun, M. Zhu and Y. Duan, *Biomaterials*, 2012, **33**, 4403-4412.

36 A. A. Dar, A. Garai, A. R. Das and S. Ghosh, *J. Phys. Chem. A*, 2010, **114**, 5083-5091.

37 S. Das, D. K. Sharma, S. Chakrabarty, A. Chowdhury and S. S. Gupta, *Langmuir*, 2015, **31**, 3402−3412.

38 S. Lv, M. Li, Z. Tang, W. Song, H. Sun, H. Liu and X. Chen, *Acta Biomater.*, 2013, **9**, 9330-9342.

39 F. Wang, D. Zhang, Q. Zhang, Y. Chen, D. Zheng, L. Hao, C. Duan, L. Jia, G. Liu and Y. Liu, *Biomaterials*, 2011, **32**, 9444-9456.

40 X. Yang, H. Hong, J. J. Grailer, I. J. Rowland, A. Javadi, S. A. Hurley, Y. Xiao, Y. Yang, Y. Zhang, R. J. Nickles, W. Cai, D. A. Steeber and S. Gong, *Biomaterials*, 2011, **32**, 4151-4160.

41 W. M. Li, C. W. Su, Y. W. Chen and S. Y. Chen, *Acta Biomater.*, 2015, **15**,

191-199.

42 X. Zeng, R. Morgenstern and A. M. Nyström, *Biomaterials*, 2014, **35**, 1227-1239.

43 D. Li, H. Sun, J. Ding, Z. Tang, Y. Zhang, W. Xu, X. Zhuang and X. Chen, *Acta Biomater.*, 2013, **9**, 8875-8884.

44 H. Xu, D. Yang, C. Cai, J. Gou, Y. Zhang, L. Wang, H. Zhong and X. Tang, *Acta Biomater.*, 2015, **16**, 156-168.

Graphic abstract

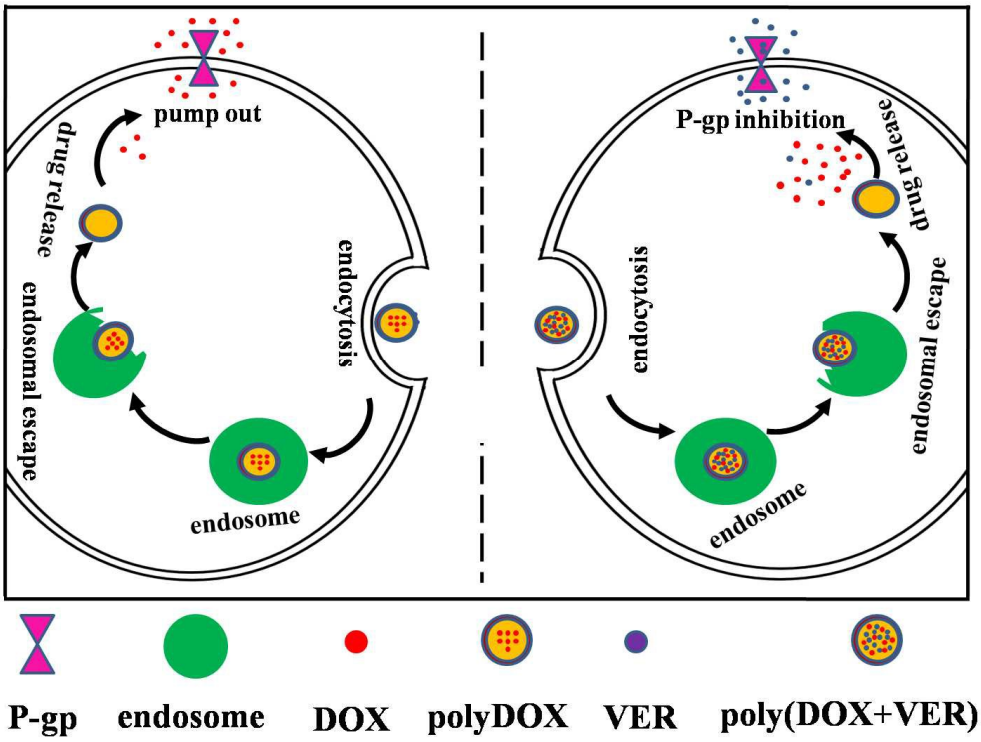

A promising co-delivery system was proposed for effectively reversing multidrug resistance of cancer cells and simultaneously improving the anticancer effect of the drug.